

Implementation of Ionic processes in SKIRT

Naoto Samehima^{1,2}, Arno Lauwers³, Bert Vander Meulen^{3,4,5},
Masahiro Tsujimoto^{1,2}, Liyi Gu⁵, Maarten Baes³, Peter Camps³

1. ISAS/JAXA 2. U. of Tokyo 3. Ghent U. 4. ESTEC/ESA 5. SRON

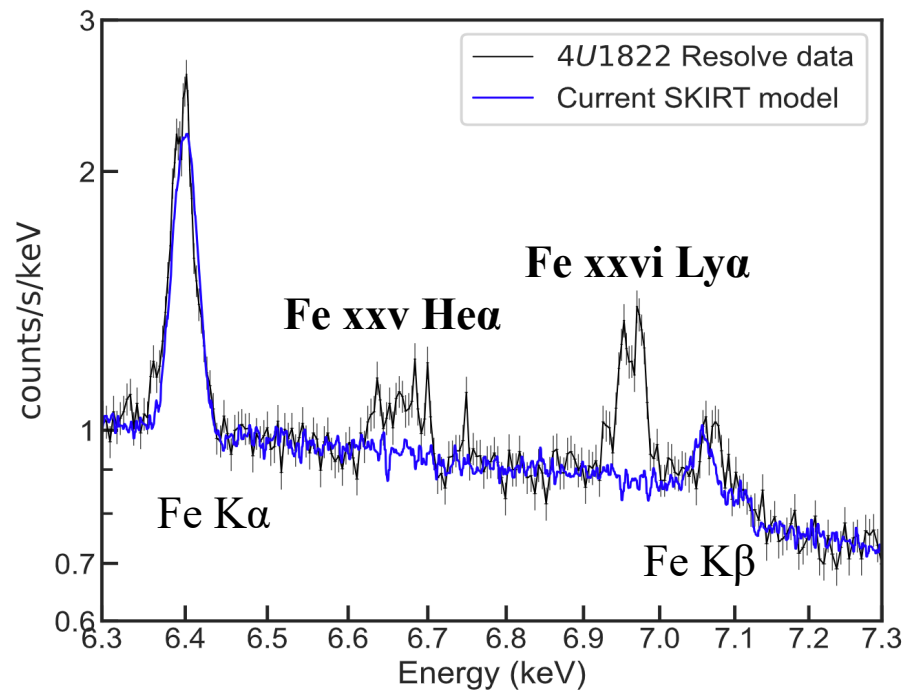
14/05/2026 @SKIRT Workshop

Outline

1. Introduction
2. Physics
 - a. Scope
 - b. Atomic processes
 - c. Formalism
3. Implementation
 - a. Resonance scattering
 - b. Radiative recombination
4. Verification
 - a. Microphysics
 - b. Radiative transfer effects
5. Demonstration
 - a. Setup
 - b. Spectra
 - c. $\text{Ly}\alpha 1/\text{Ly}\alpha 2$ ratio
6. Summary

1. Introduction

- **Processes involving ions** have not yet been implemented in SKIRT.
- X-ray spectra of compact objects are rich in numerous features arising from **highly ionized ions**.



Resolve spectrum of a LMXB (4U1822-371) and a SKIRT model.

2-a. Scope

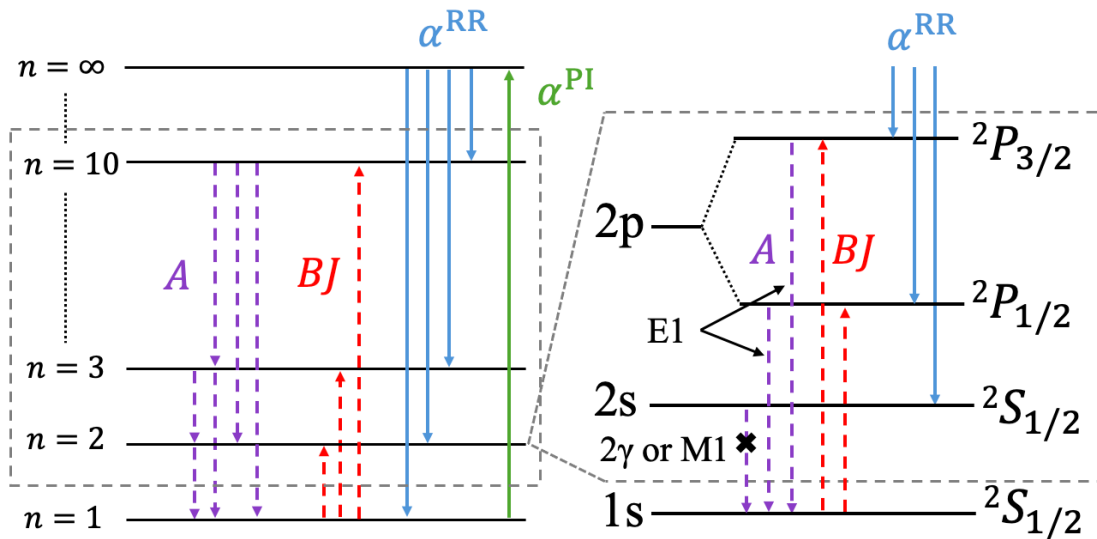
■ Current status of ionic processes in SKIRT

- Photo-absorption of all ions with $Z=1-30$ (Lauwers et al. in prep.).
- Fluorescence $K\alpha_1$ and $K\alpha_2$ lines of ions with the number of electrons $N \geq 5$ and $Z=5-30$ (Lauwers et al. in prep.).
- **Lyman-series lines of H-like ions (Sameshima et al. submitted).**
✧ Available only on the PR branch.
- He-like line complexes in progress (Sameshima et al. in prep.) .

■ We focus on the Lyman-series lines of H-like ions.

- Resonance scattering for $\text{Ly}\alpha$ line of H has been implemented in SKIRT (Camps et al. 2021).
- We make the following extensions:
 1. Other elements up to $Z = 30$.
 2. Higher Lyman series with $1 < n \leq 10$ levels.
 3. Distinguish the fine-structure levels of $\text{Ly}\alpha_1$ and $\text{Ly}\alpha_2$.
 4. Linear polarization.

2-b. Atomic processes

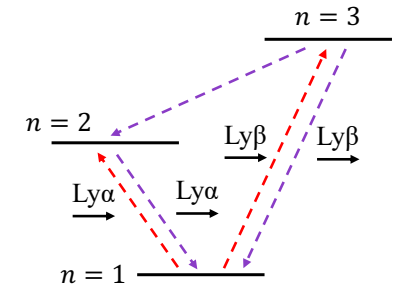


Levels and atomic processes considered in this implementation.

Population processes:

- Radiative recombination directly and in cascade through intermediate levels.
- Radiative excitation from the ground level.

※ A fraction of $\text{Ly}\beta$ degrades to $\text{Ly}\alpha$.



De-population processes:

- Radiative E1 transition for the excited levels.
- Two-photon decay (2γ) or M1 transition for the meta-stable levels.
- Photo-ionization from the ground level.

2-c. Formalism

- The rate equation for the density n_i of the excited level $i \in \{1, 2, \dots, N\}$ at a steady-state condition is given by

$$\dot{\mathbf{n}} = \mathbf{\Gamma} \mathbf{n} + \mathbf{S} = \mathbf{0}$$

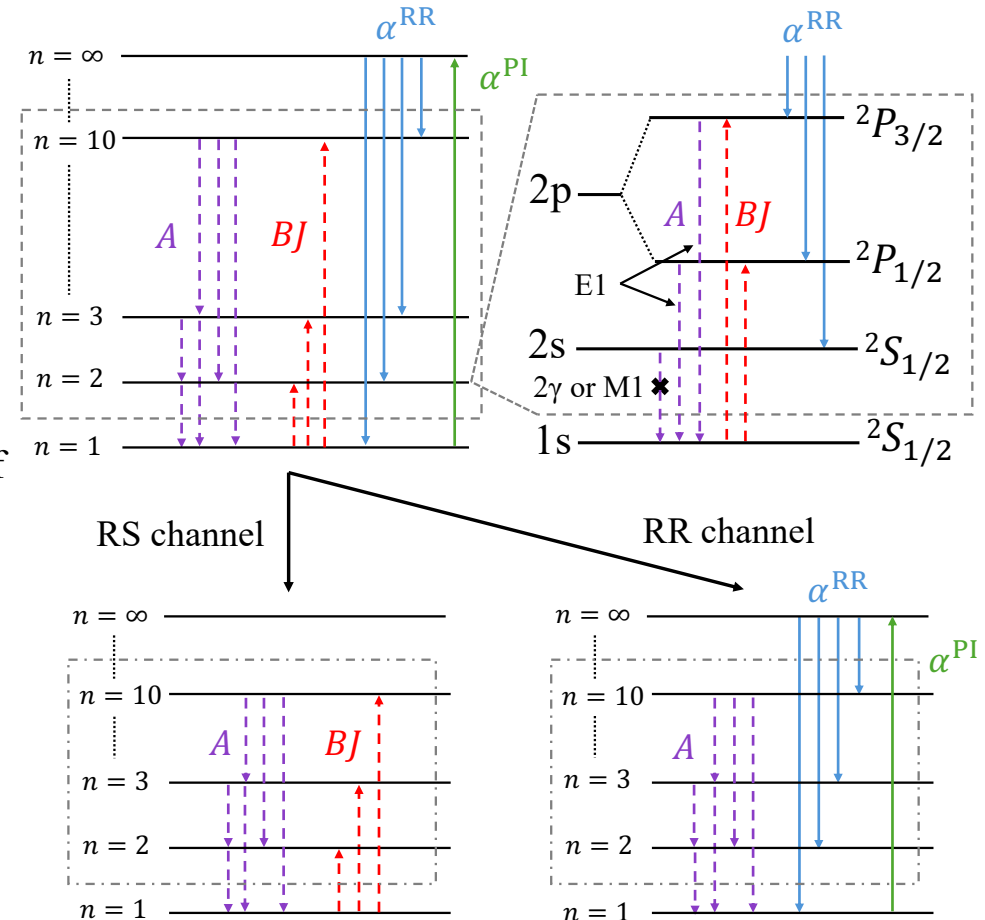
- Cascade matrix $\mathbf{\Gamma}$ with Γ_{ij} represents the **spontaneous radiative decay (A)** from the level j to i .
- Source term \mathbf{S} with S_i represents the populating rates of the level i from n_0 and n_∞ .

$$S_i = n_e n_\infty \alpha_i^{RR}(T) + n_0 B_{0i} J(\nu = \nu_{i0})$$

- We treat two channels separately:

$$\text{RS channel} \quad \mathbf{\Gamma} \mathbf{n}_{RS} + \mathbf{S}_{RS} = \mathbf{0}$$

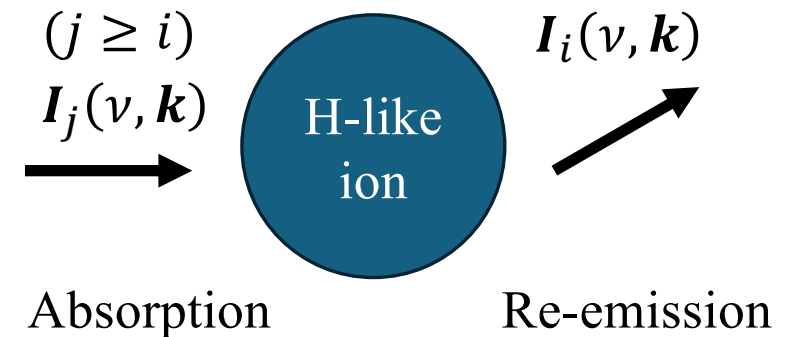
$$\text{RR channel} \quad \mathbf{\Gamma} \mathbf{n}_{RR} + \mathbf{S}_{RR} = \mathbf{0}$$



3-a. Resonance scattering

$$\frac{dI_i(\nu', \mathbf{k}')}{ds} = \sum_{j \geq i} \mathbf{R}_{ij}(\nu, \mathbf{k}, \nu', \mathbf{k}') P_{ij} \alpha_j^{\text{RS}}(\nu) I_j(\nu, \mathbf{k})$$

- $I_j(\nu, \mathbf{k})$: Stokes vector (I_j, Q_j, U_j) of photons between the ground level and the excited level j .
- α_j^{RS} : Amplitude of resonance scattering.
- P_{ij} : Branching ratio to represent the degradation probability from j to i .
- \mathbf{R}_{ij} : Matrix to represent the redistribution of frequency and direction.



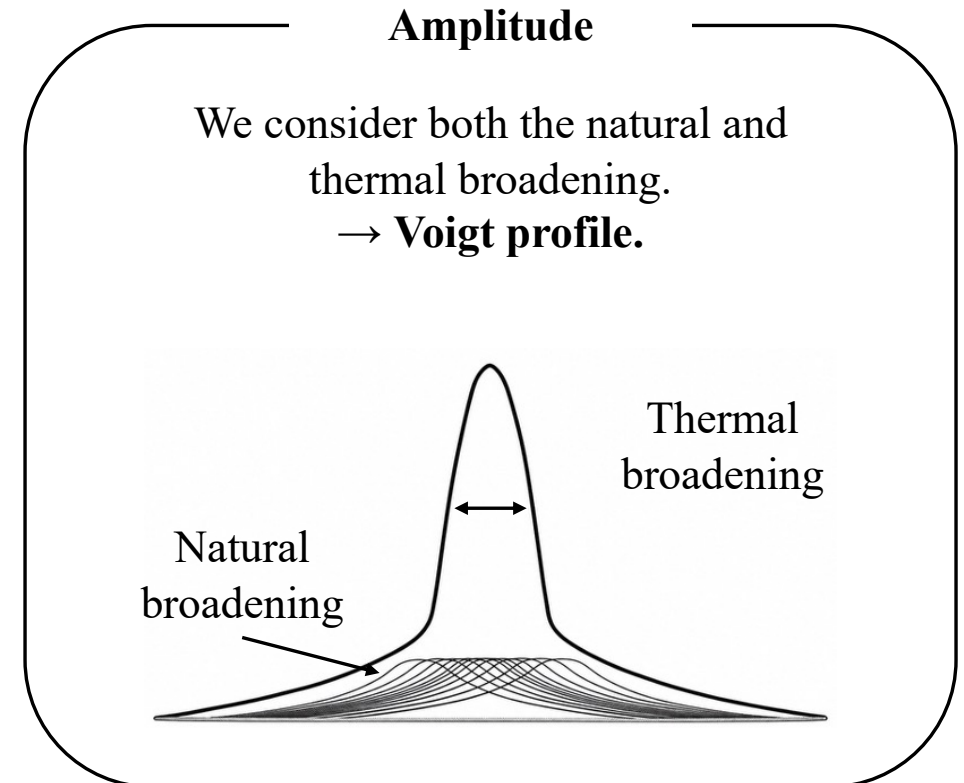
※ We retrieve the atomic data from SPEX v.3.08.01 (Kaastra et al. 2024).

3-a. Resonance scattering

$$\frac{dI_i(\nu', \mathbf{k}')}{ds} = \sum_{j \geq i} \mathbf{R}_{ij}(\nu, \mathbf{k}, \nu', \mathbf{k}') P_{ij} \alpha_j^{RS}(\nu) I_j(\nu, \mathbf{k})$$

- $I_j(\nu, \mathbf{k})$: Stokes vector (I_j, Q_j, U_j) of photons between the ground level and the excited level j .
- α_j^{RS} : **Amplitude of resonance scattering.**
- P_{ij} : Branching ratio to represent the degradation probability from j to i .
- \mathbf{R}_{ij} : Matrix to represent the redistribution of frequency and direction.

※ We retrieve the atomic data from SPEX v.3.08.01 (Kaastra et al. 2024).



3-a. Resonance scattering

$$\frac{d\mathbf{I}_i(\nu', \mathbf{k}')}{ds} = \sum_{j \geq i} \mathbf{R}_{ij}(\nu, \mathbf{k}, \nu', \mathbf{k}') P_{ij} \alpha_j^{\text{RS}}(\nu) \mathbf{I}_j(\nu, \mathbf{k})$$

- $\mathbf{I}_j(\nu, \mathbf{k})$: Stokes vector (I_j, Q_j, U_j) of photons between the ground level and the excited level i .
- α_j^{RS} : Amplitude of resonance scattering.
- P_{ij} : **Branching ratio to represent the degradation probability from j to i .**
- \mathbf{R}_{ij} : Matrix to represent the redistribution of frequency and direction.

※ We retrieve the atomic data from SPEX v.3.08.01 (Kaastra et al. 2024).

Branching ratio

- When a $0 \rightarrow j$ radiative excitation occurs, subsequent radiative cascades determine the equilibrium level population.
- To obtain the level population, we solve the rate equation in which the source term only includes **the $0 \rightarrow j$ radiative excitation rate.**

$$\mathbf{\Gamma} \mathbf{n}_{\text{RS}} + \mathbf{S}_{\text{RS}} = \mathbf{0}$$

$$S_k^{\text{RS}} = \begin{cases} n_0 B_{0j} J_j(\nu = \nu_{0j}), & k = j \\ 0, & k \neq j \end{cases}$$

- The branching ratio is given as the fraction of the $i \rightarrow 0$ transition rate over the $0 \rightarrow j$ radiative excitation rate by

$$P_{ij} = \frac{n_i A_{i0}}{n_0 B_{0j} J_j(\nu = \nu_{0j})}$$

3-a. Resonance scattering

$$\frac{dI_i(\nu', \mathbf{k}')}{ds} = \sum_{j \geq i} \mathbf{R}_{ij}(\nu, \mathbf{k}, \nu', \mathbf{k}') P_{ij} \alpha_j^{RS}(\nu) I_j(\nu, \mathbf{k})$$

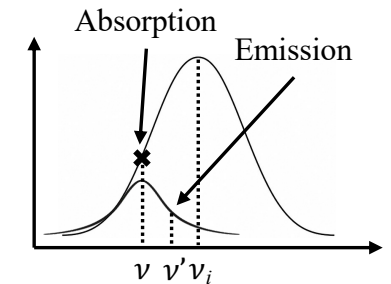
- $I_j(\nu, \mathbf{k})$: Stokes vector (I_j, Q_j, U_j) of photons between the ground level and the excited level i .
- α_j^{RS} : Amplitude of resonance scattering.
- P_{ij} : Branching ratio to represent the degradation probability from j to i .
- \mathbf{R}_{ij} : **Matrix to represent the redistribution of frequency and direction.**

※ We retrieve the atomic data from SPEX v.3.08.01 (Kaastra et al. 2024).

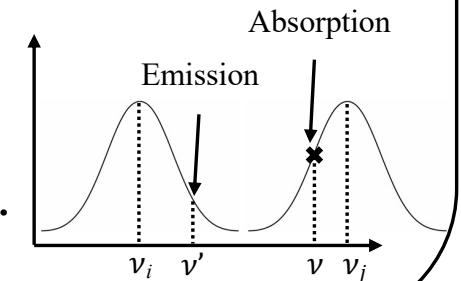
Redistribution

■ Frequency

- For RS without photon degradation ($i = j$), the absorbed and re-emitted photons are coherent.
→ **Partial redistribution.**



- For RS with photon degradation ($j > i$), the coherency does not hold.
→ **Complete redistribution.**



3-a. Resonance scattering

$$\frac{dI_i(\nu', \mathbf{k}')}{ds} = \sum_{j \geq i} \mathbf{R}_{ij}(\nu, \mathbf{k}, \nu', \mathbf{k}') P_{ij} \alpha_j^{RS}(\nu) \mathbf{I}_j(\nu, \mathbf{k})$$

- $\mathbf{I}_j(\nu, \mathbf{k})$: Stokes vector (I_j, Q_j, U_j) of photons between the ground level and the excited level i .
- α_j^{RS} : Amplitude of resonance scattering.
- P_{ij} : Branching ratio to represent the degradation probability from j to i .
- \mathbf{R}_{ij} : **Matrix to represent the redistribution of frequency and direction.**

※ We retrieve the atomic data from SPEX v.3.08.01 (Kaastra et al. 2024).

Redistribution

■ Direction

- Redistribution function is different for the three Stokes parameters. $\rightarrow 3 \times 3$ **Müller matrix**.
- Linear combination of monopole and dipole distribution, depending on the quantum number J and ΔJ (Hamilton 1947).

$$\begin{aligned} \mathbf{M}(\theta) &= E_1 \mathbf{M}^{(m)}(\theta) + E_2 \mathbf{M}^{(d)}(\theta) \\ &= E_1 \frac{1}{2} \begin{pmatrix} 1 & 0 & 0 \\ 0 & 0 & 0 \\ 0 & 0 & 0 \end{pmatrix} \\ &\quad + E_2 \frac{3}{8} \begin{pmatrix} 1 + \cos^2 \theta & -\sin^2 \theta & 0 \\ -\sin^2 \theta & 1 + \cos^2 \theta & 0 \\ 0 & 0 & 2 \cos \theta \end{pmatrix} \end{aligned}$$

- Ly α_1 ($J = 1/2, \Delta J = 1$) $\rightarrow E_1 = E_2 = 1/2$.
- Ly α_2 ($J = 1/2, \Delta J = 0$) $\rightarrow E_1 = 1, E_2 = 0$.
- RS with photon degradation $\rightarrow E_1 = 1, E_2 = 0$.

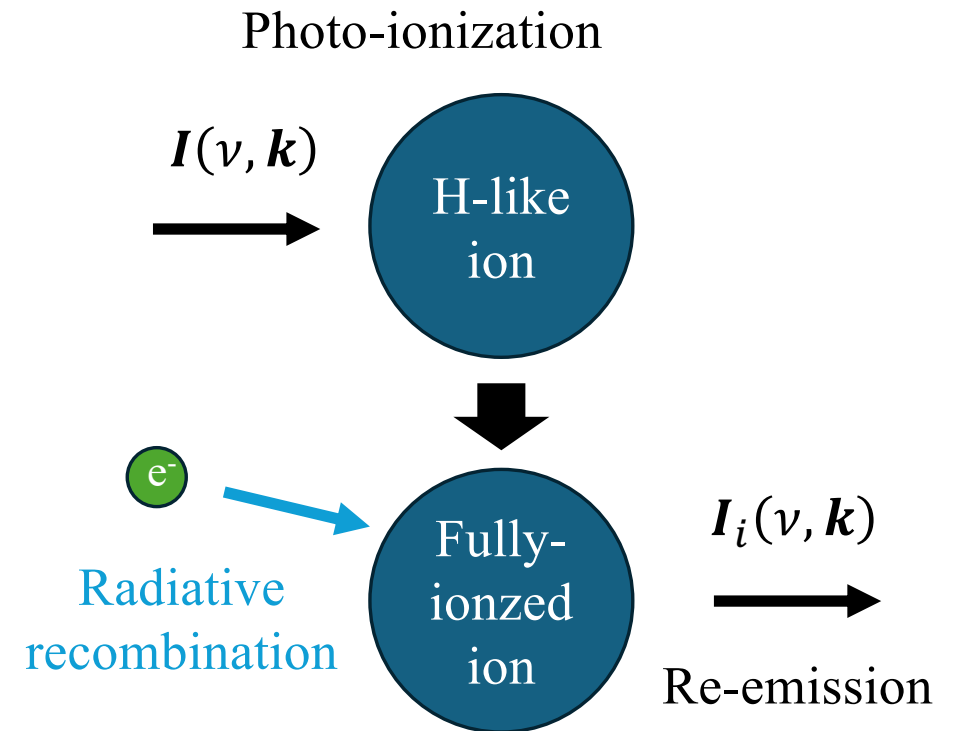


3-b. Radiative recombination

$$\frac{d\mathbf{I}_i(\nu', \mathbf{k}')}{ds} = \mathbf{R}_i(\nu, \mathbf{k}, \nu', \mathbf{k}') P_i \alpha^{\text{PI}}(\nu) \mathbf{I}(\nu, \mathbf{k})$$

- $\mathbf{I}(\nu, \mathbf{k})$: Stokes vector (I, Q, U) of ionizing photons.
- α^{PI} : Amplitude of photo-ionization.
- P_i : Branching ratio that a single photo-ionization event yields a Lyman $i \rightarrow 0$ photon.
- \mathbf{R}_i : Matrix to represent the redistribution of frequency and direction.

※ We retrieve the atomic data from SPEX v.3.08.01 (Kaastra et al. 2024).



3-b. Radiative recombination

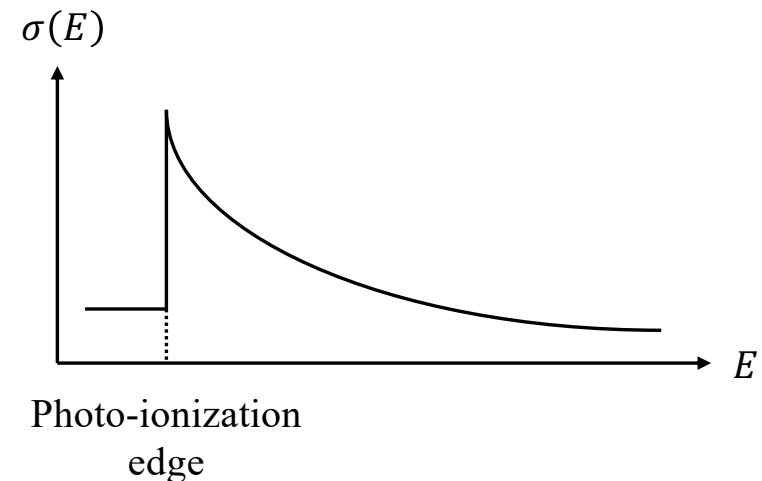
$$\frac{dI_i(\nu', \mathbf{k}')}{ds} = \mathbf{R}_i(\nu, \mathbf{k}, \nu', \mathbf{k}') P_i \alpha^{\text{PI}}(\nu) I(\nu, \mathbf{k})$$

- $I(\nu, \mathbf{k})$: Stokes vector (I, Q, U) of ionizing photons.
- α^{PI} : **Amplitude of photo-ionization.**
- P_i : Branching ratio that a single photo-ionization event yields a Lyman $i \rightarrow 0$ photon.
- \mathbf{R}_i : Matrix to represent the redistribution of frequency and direction.

※ We retrieve the atomic data from SPEX v.3.08.01 (Kaastra et al. 2024).

Amplitude

Verner & Yakovlev (1995) provided a parametrized description of **the photo-ionization cross-section for the ground state of H-like ions.**



3-b. Radiative recombination

$$\frac{d\mathbf{I}_i(\nu', \mathbf{k}')}{ds} = \mathbf{R}_i(\nu, \mathbf{k}, \nu', \mathbf{k}') P_i \alpha^{\text{PI}}(\nu) \mathbf{I}(\nu, \mathbf{k})$$

- $\mathbf{I}(\nu, \mathbf{k})$: Stokes vector (I, Q, U) of ionizing photons.
- α^{PI} : Amplitude of photo-ionization.
- P_i : **Branching ratio that a single photo-ionization event yields a Lyman $i \rightarrow 0$ photon.**
- \mathbf{R}_i : Matrix to represent the redistribution of frequency and direction.

※ We retrieve the atomic data from SPEX v.3.08.01 (Kaastra et al. 2024).

Branching ratio

- When a fully-ionized ion recombines with an electron, subsequent radiative cascades determine the equilibrium level population.
- To obtain the level population, we solve the rate equation in which the source term is the **level-resolved radiative recombination rate** $\alpha_i^{\text{RR}}(T)$ from Mao & Kaastra (2016).

$$\mathbf{\Gamma} \mathbf{n}_{\text{RR}} + \mathbf{S}_{\text{RR}} = \mathbf{0}$$

$$S_i^{\text{RR}} = n_e n_\infty \alpha_i^{\text{RR}}(T)$$

- The branching ratio is given as the fraction of the $i \rightarrow 0$ transition rate over the total recombination rate by

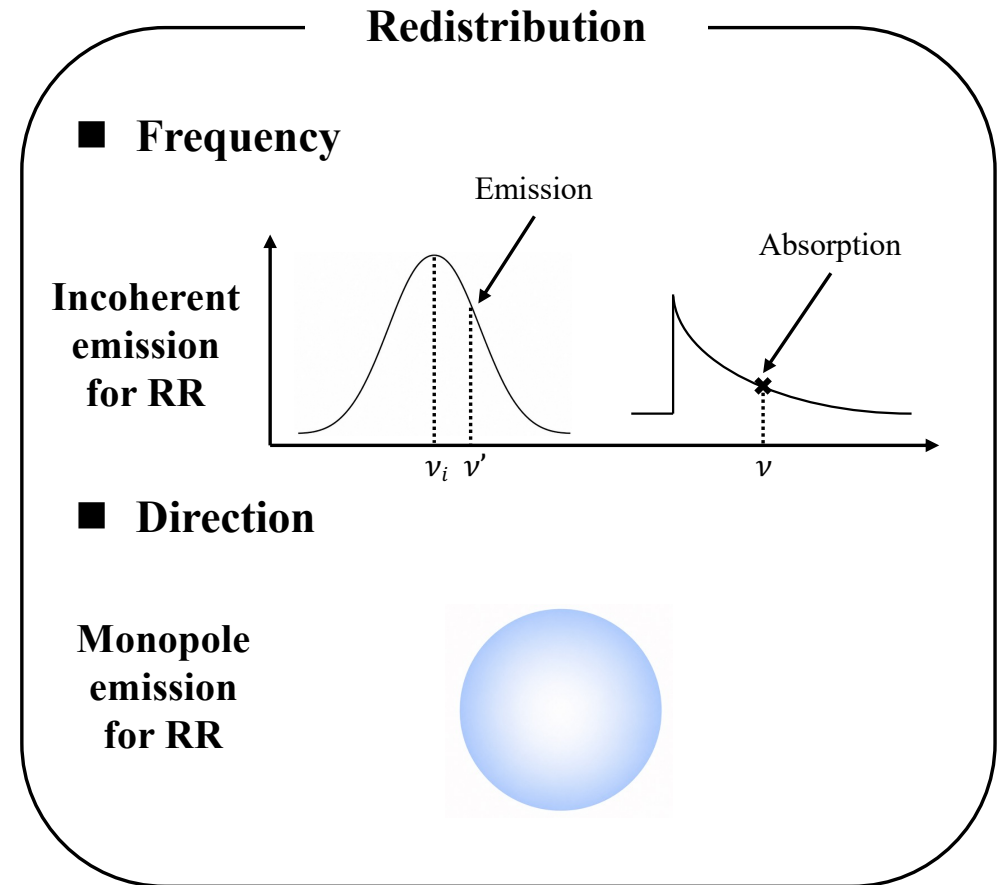
$$P_i = \frac{n_i A_{i0}}{n_e n_\infty \sum_k \alpha_k^{\text{RR}}(T)}$$

3-b. Radiative recombination

$$\frac{dI_i(\nu', \mathbf{k}')}{ds} = R_i(\nu, \mathbf{k}, \nu', \mathbf{k}') P_i \alpha^{\text{PI}}(\nu) I(\nu, \mathbf{k})$$

- $I(\nu, \mathbf{k})$: Stokes vector (I, Q, U) of ionizing photons.
- α^{PI} : Amplitude of photo-ionization.
- P_i : Branching ratio that a single photo-ionization event yields a Lyman $i \rightarrow 0$ photon.
- R_i : **Matrix to represent the redistribution of frequency and direction.**

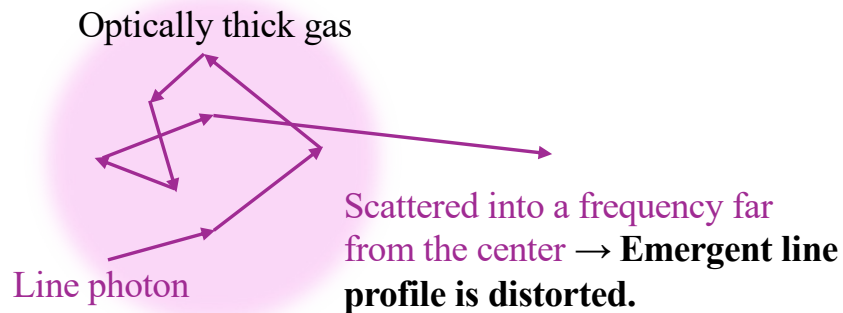
※ We retrieve the atomic data from SPEX v.3.08.01 (Kaastra et al. 2024).



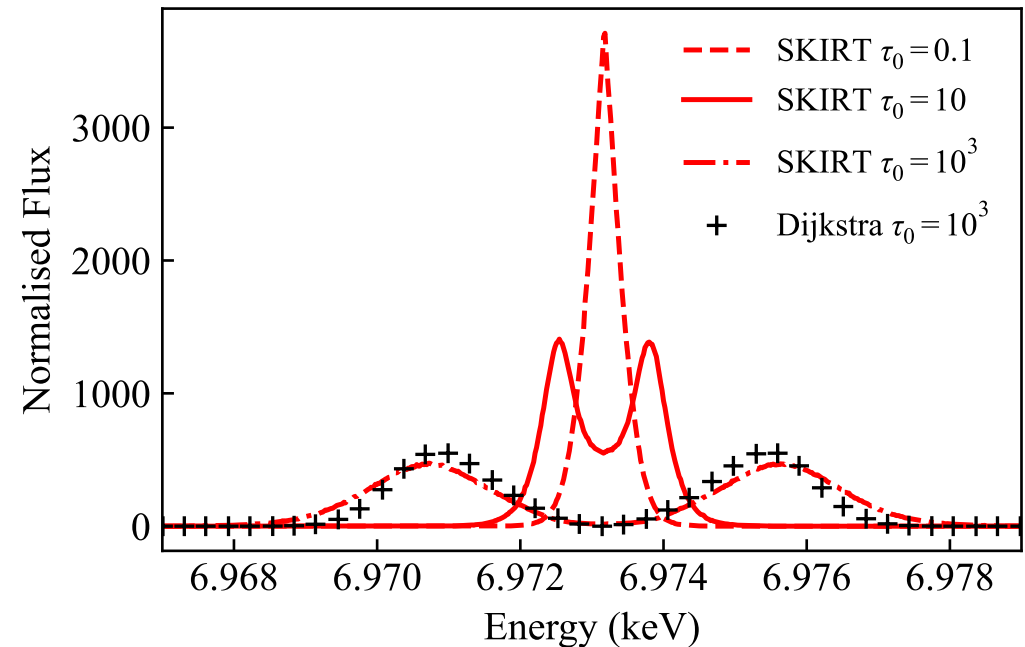
4-b. Radiative transfer effects (1/3)

■ Distortion of line profile

- The emergent line profile can be distorted by frequency redistribution, **which is not captured by 1D-RT models that use the escape-probability approximation.**



- We obtained the Fe Ly α_1 line profile with $\tau_0 = 0.1, 10, 10^3$ with SKIRT.
- The SKIRT result for $\tau_0 = 10^3$ is close to an asymptotic expression by Dijkstra et al. (2006).



Ly α_1 line profile calculated using SKIRT for $\tau_0 = 0.1, 10, 10^3$.

5-a. Setup

- We make a demonstration for a more realistic setup.

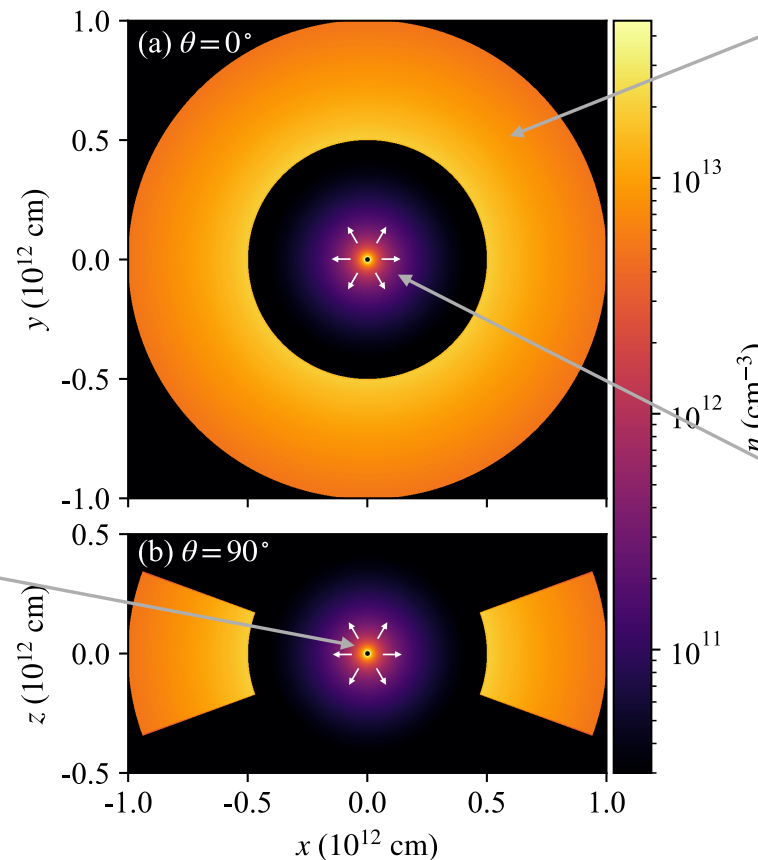
→ **LMXB consisting of a cold outer disk and a hot outflowing wind.**

Source

- Point-like.
- Multi-temperature blackbody.
- Anisotropic emission from an inner accretion disk (Netzer 1987).

$$L(\theta) \propto \begin{cases} \cos \theta (2 \cos \theta + 1), & 0 \leq \theta \leq \frac{\pi}{2}, \\ \cos \theta (2 \cos \theta - 1), & \frac{\pi}{2} \leq \theta \leq \pi. \end{cases}$$

Density distribution.



Outer disk

- Neutral atoms with a solar abundance.
- Opening angle 20° .
- **Block the emission from the wind at the edge-on.**

Outflowing wind

- Ion density calculated with Cloudy.
- Radial velocity of 100 km/s.
- **Production site of Lyman-series lines.**

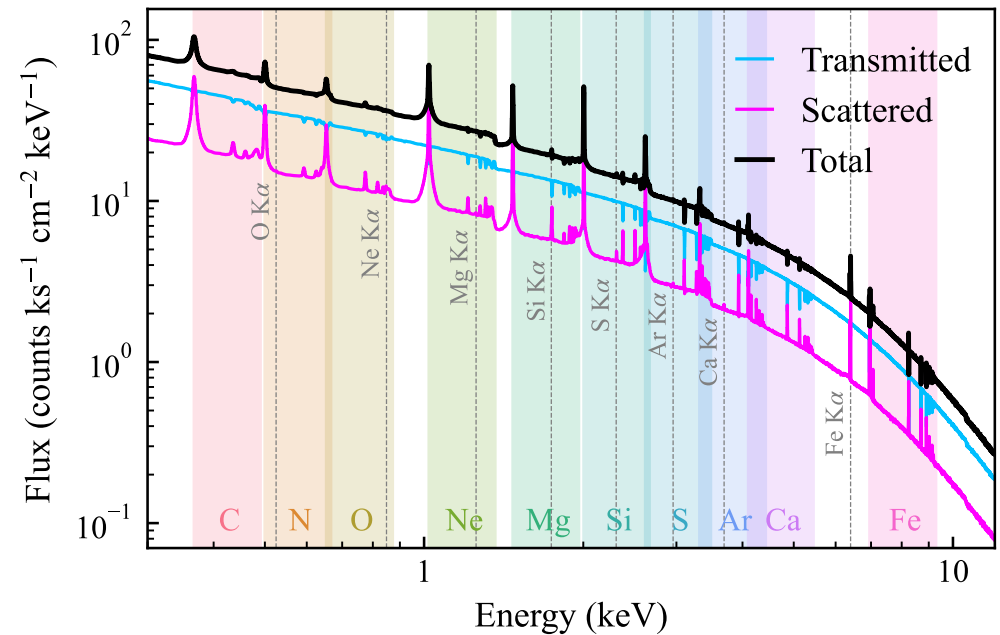
5-b. Spectra

■ Overall spectra

- **Transmitted**: Continuum attenuation by electron scattering, together with absorption lines and edges by H-like ions.
- **Scattered**: Lyman-series lines as well as fluorescence lines by neutral atoms.

■ Close-up view of the Fe Ly α doublet

- P Cygni profiles at $\theta = 30^\circ$ and 60° .
- The **transmitted** component is completely lost and only the **emission line** is observed at $\theta = 90^\circ$.



Overall spectra synthesized with SKIRT at $\theta = 60^\circ$.

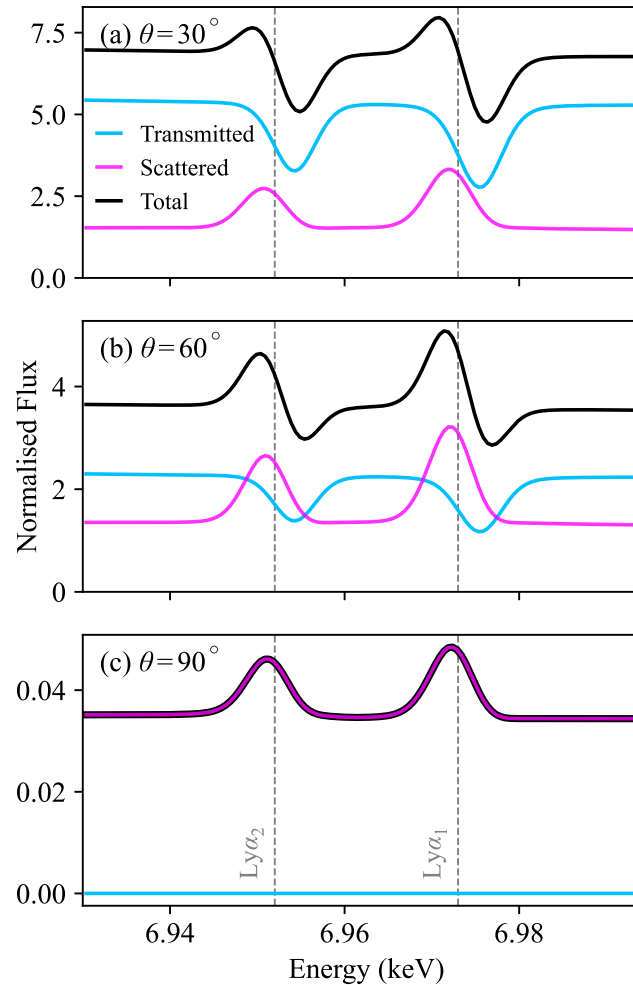
5-b. Spectra

■ Overall spectra

- **Transmitted**: Continuum attenuation by electron scattering, together with absorption lines and edges by H-like ions.
- **Scattered**: Lyman-series lines as well as fluorescence lines by neutral atoms.

■ Close-up view of the Fe $\text{Ly}\alpha$ doublet

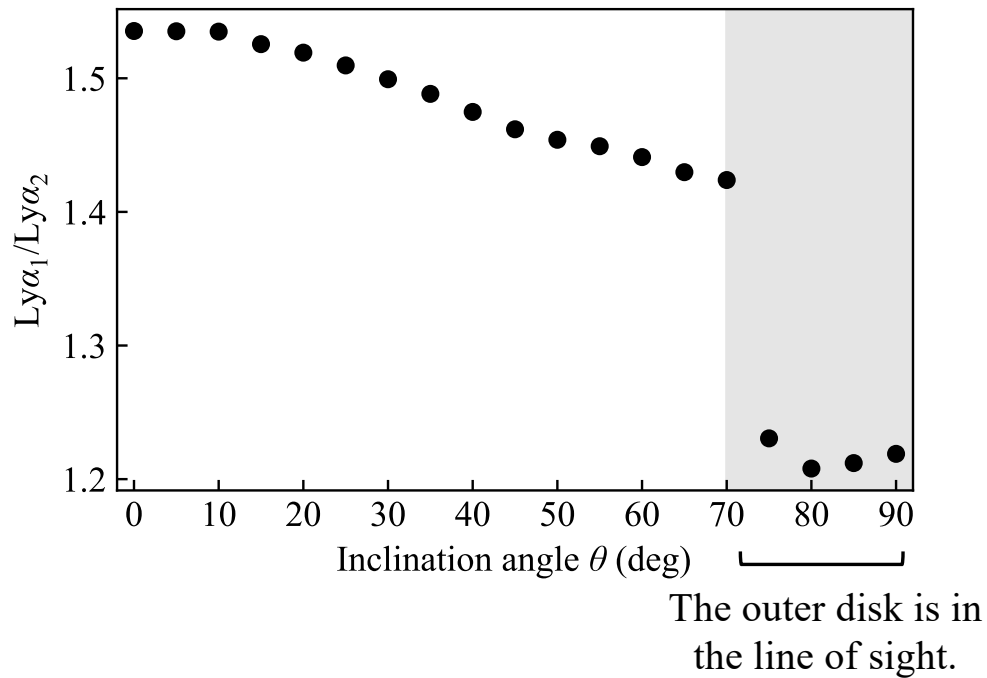
- P Cygni profiles at $\theta = 30^\circ$ and 60° .
- The **transmitted** component is completely lost and only the **emission line** is observed at $\theta = 90^\circ$.



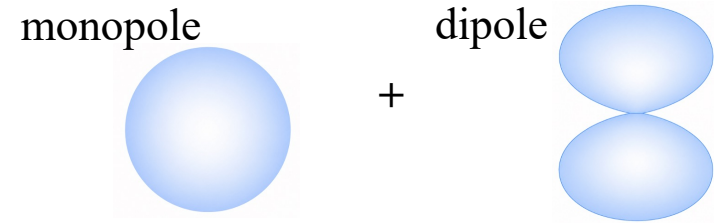
Close-up view of the Fe $\text{Ly}\alpha$ doublet at different viewing angles.

5-c. Ly α_1 /Ly α_2 ratio

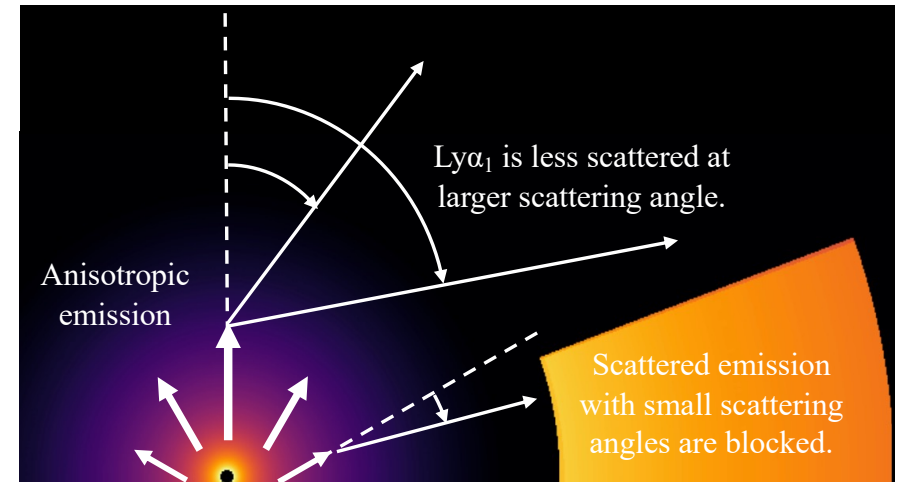
- The doublet ratio decreases as θ increases because of scattering phase function effects.



- Ly α_1 scattering phase function:



- Scattering becomes less likely at larger θ .
- Anisotropic emission and shielding by the outer disk enhance this effect.



6. Summary

1. **Motivation:** To interpret reprocessed X-ray emission from photo-ionized plasmas around compact objects, observed by XRISM and IXPE.
2. **Method:** We have implemented the Lyman-series lines H-like ions in the MC-RT code SKIRT.
3. **Implementation:**
 - a. Atomic processes: Resonant scattering (RS) and Radiative recombination (RR)
 - b. Microphysics: Cross-section, Branching ratio and Redistribution
4. **Verification:**
 - a. The implemented microphysics show good agreement with Cloudy.
 - b. The code successfully reproduces RT effects (line-profile distortion, Lyman decrement, and P Cygni profiles).
5. **Demonstration:** Anisotropy of the radiation field, geometry, and velocity structure significantly affect observable features in the spectra (P Cygni profile and the Ly α fine-structure doublet ratio).